Cardiovascular Research (2016) **111**, 204–216
doi:10.1093/cvr/cvw101

Endothelial deletion of protein tyrosine phosphatase-1B protects against pressure overload-induced heart failure in mice

Rajinikanth Gogiraju[1], Marco R. Schroeter[1], Magdalena L. Bochenek[2,3], Astrid Hubert[2], Thomas Münzel[2], Gerd Hasenfuss[1], and Katrin Schäfer[1,2]*

[1]Department of Cardiology and Pneumology, University Medical Center Göttingen, Göttingen, Germany; [2]Center for Cardiology, Department of Cardiology I, University Medical Center Mainz, Mainz, Germany; and [3]Center for Thrombosis and Hemostasis, University Medical Center Mainz, Mainz, Germany

Received 3 November 2015; revised 24 April 2016; accepted 27 April 2016; online publish-ahead-of-print 20 May 2016

Time for primary review: 23 days

Aims Cardiac angiogenesis is an important determinant of heart failure. We examined the hypothesis that protein tyrosine phosphatase (PTP)-1B, a negative regulator of vascular endothelial growth factor (VEGF) receptor-2 activation, is causally involved in the cardiac microvasculature rarefaction during hypertrophy and that deletion of PTP1B in endothelial cells prevents the development of heart failure.

Methods and results Cardiac hypertrophy was induced by transverse aortic constriction (TAC) in mice with endothelial-specific deletion of PTP1B (End.PTP1B-KO) and controls (End.PTP1B-WT). Survival up to 20 weeks after TAC was significantly improved in mice lacking endothelial PTP1B. Serial echocardiography revealed a better systolic pump function, less pronounced cardiac hypertrophy, and left ventricular dilation compared with End.PTP1B-WT controls. Histologically, banded hearts from End.PTP1B-KO mice exhibited increased numbers of PCNA-positive, proliferating endothelial cells resulting in preserved cardiac capillary density and improved perfusion as well as reduced hypoxia, apoptotic cell death, and fibrosis. Increased relative VEGFR2 and ERK1/2 phosphorylation and greater eNOS expression were present in the hearts of End.PTP1B-KO mice. The absence of PTP1B in endothelial cells also promoted neovascularization following peripheral ischaemia, and bone marrow transplantation excluded a major contribution of Tie2-positive haematopoietic cells to the improved angiogenesis in End.PTP1B-KO mice. Increased expression of caveolin-1 as well as reduced NADPH oxidase-4 expression, ROS generation and TGFβ signalling were observed and may have mediated the cardioprotective effects of endothelial PTP1B deletion.

Conclusions Endothelial PTP1B deletion improves cardiac VEGF signalling and angiogenesis and protects against chronic afterload-induced heart failure. PTP1B may represent a useful target to preserve cardiac function during hypertrophy.

Keywords Angiogenesis • Fibrosis • Heart failure • Hypertrophy • PTP1B

1. Introduction

Clinical and preclinical evidence suggests that inadequate cardiac angiogenesis is an important determinant of heart failure.[1] It is regulated by angiogenic growth factors released from stretched or hypoxic cardiomyocytes and/or fibroblasts, which interact with their specific receptors on neighbouring endothelial cells.[2] Vascular endothelial growth factor (VEGF) is essential for cardiac angiogenesis, as shown in mice with cardiomyocyte-specific deletion,[3] inducible sequestration,[4] or blockade[5] of VEGF.

Cardiac hypertrophy is initially associated with an increased capillary density, whereas a reduction in the cardiac microvasculature is observed at later stages, in mismatch with the elevated oxygen and nutrient demands of the hypertrophied cardiomyocytes. The molecular mechanisms underlying the insufficient adaptive cardiac angiogenesis in chronic cardiac hypertrophy are not fully understood and may include the inadequate expression of angiogenic growth factors. For example, a reduced cardiac expression of VEGF has been reported in patients with dilative cardiomyopathy and heart failure,[6] whereas levels of the VEGF antagonist soluble VEGF receptor-1 were found to be

* Corresponding author. Center for Cardiology, Cardiology I, University Medical Center of the Johannes Gutenberg University, Mainz, Germany. Tel: +49 6131 17 4221; fax: +49 6131 17 5660, E-mail: katrin.schaefer@unimedizin-mainz.de

increased.[7] On the other hand, elevated placental growth factor levels have been detected in serum of patients with ischaemic heart failure,[8] suggesting that a reduced responsiveness of coronary endothelial cells towards angiogenic growth factor stimulation may also be involved in the observed rarefaction of the cardiac microvasculature.

Angiogenic growth factors signal via tyrosine kinase receptors, whose activity is controlled by protein tyrosine phosphatases (PTPs) and the dephosphorylation of specific phosphotyrosine residues. A major PTP expressed in endothelial cells is PTP1B. Previous studies demonstrated an increased PTP1B expression in response to peripheral ischaemia and showed that PTP1B overexpression inhibits the VEGF-induced autophosphorylation of VEGFR2, whereas siRNA-mediated knockdown or endothelial cell-specific deletion of PTP1B improved VEGF signal transduction and angiogenesis.[9,10]

The role of PTP1B in the heart has so far been primarily examined in mouse models of chronic myocardial infarction. For example, systemic pharmacological inhibition or genetic deletion of PTP1B was shown to protect mice against chronic heart failure induced by myocardial infarction,[11] and also was found to improve the peripheral endothelial dysfunction in mice with post-ischaemic heart failure.[12] However, PTP1B is widely expressed in many tissues, and systemic inhibition or deletion may have influenced other cell types and parameters important for the cardiac remodelling response. Thus, the importance of endothelial PTP1B during cardiac hypertrophy and the development of heart failure are unknown. Here, we examined the hypothesis that PTP1B expressed in endothelial cells is causally involved in the reduced cardiac vascularization and impaired angiogenic signal transduction in the failing heart following chronically elevated cardiac afterload, and that endothelial PTP1B overexpression promotes the progression towards heart failure.

2. Methods

2.1 Experimental animals

To generate mice with inducible endothelial cell-specific PTP1B deletion (End.PTP1B-KO), mice with loxP-flanked (floxed, fl) PTP1B alleles (C57BL/6 background; courtesy of Benjamin G. Neel)[13] were mated with mice expressing a Cre recombinase-estrogen receptor fusion protein ER(T2) under control of the endothelial receptor tyrosine kinase (Tie2) promoter (C57BL/6 background; courtesy of Bernd Arnold).[14] Genotyping and detection of deleted PTP1B alleles (delta PTP1B) were performed as described.[13,14] Cre recombinase activity was induced by feeding 5–6 weeks old mice with rodent chow containing tamoxifen citrate (TD55125; Harlan Teklad) over 6 weeks. Cre-wild-type (WT) × $PTP1B^{fl/fl}$ littermates fed tamoxifen chow served as controls (End.PTP1B-WT). Age- and gender-matched littermates were used throughout the study. The investigation conforms to the Guide for the Care and Use of Laboratory Animals published by the US National Institutes of Health (NIH Publication No. 85-23, revised 1985 and updated 2011). All animal care and experimental procedures had been approved by the institutional Animal Research Committee and complied with national guidelines for the care and use of laboratory animals.

2.2 Blood pressure measurements

Systolic and diastolic blood pressure was obtained in awake mice using a tail cuff non-invasive blood pressure system (CODA™ Monitor; Kent Scientific Corporation). A minimum of five measurements were obtained from each mouse.

2.3 Transverse aortic constriction

Female mice were anaesthetized via 2% isoflurane inhalation and subjected to minimally invasive transverse aortic constriction (TAC) surgery over a 26-gauge needle.[15] Anaesthesia depth was monitored by observing the respiratory rate and the toe-pinch reflex. Sham-operated mice, in which the aortic arch was exposed, but not ligated, were also examined. Three days after the surgery, the pressure gradient over the aortic ligature was determined using pulsed-wave Doppler. At 7 days or 20 weeks after the TAC surgery, mice were sacrificed by overdose isoflurane inhalation, and the hearts and lungs were excised and weighed. The atria were removed, and the ventricles were immediately processed for RNA and protein isolation or cryo-embedding.

2.4 Echocardiography

Two-dimensional (2D) echocardiography was performed in mice under 1.5% isoflurane anaesthesia (Vevo 2100; Visualsonics), as described.[15] M-mode recordings were used to determine the end-diastolic (EDD) and end-systolic (ESD) LV chamber diameter and anterior (AWTh) and posterior wall thicknesses (PWTh). Fractional shortening (FS) was calculated as (EDD − ESD)/EDD × 100.

2.5 Unilateral hindlimb ischaemia

New vessel formation *in vivo* was examined using the unilateral hindlimb ischaemia mouse model.[16] For surgery, male mice were anaesthetized by intraperitoneal injection of xylazine/ketamine hydrochloride. Perfusion was determined before and at the indicated time points after surgery via laser Doppler perfusion imaging (LDPI; PeriScan PIM III; Perimed) using the contralateral hindlimb as internal control (set at 100%). Four weeks later, mice were sacrificed by overdose isoflurane inhalation and the gastrocnemic muscle of the injured and the contralateral leg embedded in TissueTek® compound and processed for immunofluorescence microscopy analysis of CD31-positive cells.

2.6 Bone marrow transplantation

End.PTP1B-WT mice were sublethally irradiated and transplanted with whole bone marrow homogenates from either End.PTP1B-WT or End.PTP1B-KO littermates, essentially performed, as described.[17] Donor mice were sacrificed by overdose inhalation of isoflurane. Following a recovery period of 6 weeks, mice were subjected to unilateral hindlimb ischaemia, as described above.

2.7 Histochemistry

Histochemical analyses were performed on 5 μm-thick frozen, acetone-fixed cross sections. Cardiac fibrosis was determined by Masson's trichrome (MTC) staining. Capillary endothelial cells were assessed using monoclonal antibodies against CD31 (Santa Cruz Biotechnology), followed by Cy3-labelled secondary antibodies (Molecular Probes). Cell nuclei were visualized using 4′,6-diamidino-2-phenylindole (DAPI; Sigma). In some mice, the functionality of cardiac vessels was assessed by intracardiac (i.c.) injection of endothelial fluorescein (FITC)-conjugated *Griffonia simplicifolia* isolectin B4 (GSL-I; Vector Laboratories) 15 min prior to sacrifice. PTP1B expression was assessed using monoclonal antibodies (NovusBiologicals), endothelial NO synthase expression was detected using antibodies against eNOS (Cell Signaling Technology), and TGFβ signalling was examined using antibodies against phospho-Smad2 (Ser465/467; Merck Millipore). Results are expressed as immunopositive area per mm^2. Cardiomyocyte membranes were marked using FITC-labelled wheat germ agglutinin (WGA; Molecular Probes) followed by determination of the single cardiomyocyte CSA. Per cross section, at least 10 randomly selected cardiomyocytes were evaluated and results averaged. Cardiac apoptosis was examined using terminal deoxynucleotidyl transferase dUTP nick end labelling (TUNEL; Roche). Proliferating cells were visualized using antibodies against proliferating cell nuclear antigen (PCNA; abcam). Leucocytes were detected using antibodies against murine CD45 (Santa Cruz Biotechnology). Positive cells were manually counted in 3–5 random 400X microscope fields per section, averaged per mouse, and expressed per mm^2 or per cardiomyocyte.

Hypoxia was examined using antibodies against mouse carbonate dehydratase IX (CAIX; Bioss Antibodies), reactive oxygen species using dihydroethidium (DHE; Life Technologies). Morphometric analyses were performed using image analysis software (Image ProPlus, version 4.01).

2.8 Quantitative *real-time* polymerase chain reaction

Total RNA was isolated using RNAWiz (Ambion), and the amount and quality were checked by spectrophotometry (Nanodrop; Thermo Scientific). One microgram of RNA was reverse-transcribed into cDNA, followed by quantitative polymerase chain reaction (qPCR) using real-time assessment of SYBR® Green (Applied Biosystems) and the iCycler iQ Detection system (BioRad). Primers and qPCR conditions are listed in Supplementary material online, *Table S1*. Results were calculated using the delta Ct method and normalized to glyceraldehyde-3-phosphate dehydrogenase (GAPDH) RNA and are reported as -fold change vs. sham-operated mice. In preliminary analyses, cardiac expression of GAPDH was tested and found not to be affected by the genotype or the surgical intervention.

2.9 Western blot analysis

Frozen spleen and heart tissue was pulverized on liquid nitrogen and resuspended in lysis buffer containing fresh protease and phosphatase inhibitors. Equal amounts of protein (40 μg) were fractionated by sodium dodecyl sulfate polyacrylamide gel electrophoresis together with molecular weight standards and transferred to nitrocellulose membranes (Protran®, Whatman). Membranes were blocked in 5% bovine serum albumin (in Tris-buffered saline, containing 0.1% Tween-20), followed by incubation with antibodies against AKT (phosphorylated at Ser43 and total), caveolin-1 (phosphorylated at Tyr14 and total), eNOS (phosphorylated at Ser1177 and total), ERK1/2 (phosphorylated at Thr202/Tyr204 and total), PDGFRβ (phosphorylated at Tyr751 and total), VEGFR2 (phosphorylated at Tyr996 and total; all Cell Signaling Technology), or against FGFR1 (phosphorylated at Tyr653/654 and total; ThermoScientific), HIF1α (abcam), NOX4 (abcam), and PTP1B (Novus Biologicals). Protein bands were visualized using horseradish peroxidase-conjugated secondary antibodies (Amersham Biosciences), followed by detection with SuperSignal® West Pico Substrate (Pierce). Protein bands were quantified by densitometry and normalized to GAPDH (HyTest Ltd) protein. Results are expressed as -fold change vs. sham-operated mice of the same genotype run on the same gel.

2.10 Statistical analysis

Quantitative data are presented as mean ± SEM. Normal distribution was confirmed for all data sets using the D'Agostino and Pearson omnibus normality test. Differences were compared using ANOVA test (or repeated measures ANOVA for findings in the same animal before and after an intervention) followed by Bonferroni's multiple comparison test. Frequencies were compared using the χ^2 test. Survival analysis was performed using the log-rank test. Statistical significance was assumed if P reached a value of <0.05. All analyses were performed using data analysis software (GraphPad Software, Inc.; version 6.0).

3. Results

3.1 Generation of mice with conditional deletion of PTP1B in endothelial cells

Mice with inducible endothelial cell-specific deletion of PTP1B (End.PTP1B-KO) were generated as described in the Methods section. Tie2.ERT2.Cre mice have been shown to allow efficient temporal gene deletion exclusively in endothelial cells, including the heart, whereas the percentage of recombined cells was found to be negligible in haematopoietic cells.[14] Following the induction of Cre recombinase activity by feeding mice tamoxifen-containing rodent chow, PTP1B gene excision was confirmed by PCR analysis of genomic DNA isolated from tail biopsies (Supplementary material online, *Figure SIA*) and total heart homogenates (Supplementary material online, *Figure SIB*). Immunofluorescence analysis followed by confocal microscopy revealed low PTP1B expression in the sham-operated mouse hearts of both genotypes, whereas the observed increase in endothelial PTP1B expression in the banded hearts of End.PTP1B-WT mice was not detected in their End.PTP1B-KO counterparts (Supplementary material online, *Figure SIC*). Western blot analysis of spleen homogenates revealed similar PTP1B protein levels in End.PTP1B-WT and End.PTP1B-KO mice (Supplementary material online, *Figure SID*).

3.2 Endothelial PTP1B deletion improves survival and cardiac function after TAC

To induce cardiac hypertrophy, mice were subjected to TAC. Longitudinal observations over 20 weeks after surgery revealed a significantly improved survival in mice lacking endothelial PTP1B: 18 out of 40 End.PTP1B-KO mice died (45%) compared with 26 out of 49 End.PTP1B-WT mice (53%) and 0 out of 11 sham-operated mice (*Figure 1A*). Of note, mice that died within the first 48 h after surgery (i.e. 8 End.PTP1B-KO mice and 23 End.PTP1B-WT mice) were excluded from this calculation to minimize any direct and acute effects of the surgical intervention on death.

Serial echocardiographic measurements revealed a significantly improved FS in mice lacking PTP1B in endothelial cells (*Figure 1B*). End.PTP1B-KO mice also exhibited significantly smaller end-diastolic (*Figure 1C*) and end-systolic (*Figure 1D*) LV dimensions. The PWTh increased to a similar extent after TAC in both genotypes (not shown). Endothelial PTP1B deletion also was associated with a lower mean heart-to-body weight ratio (*Figure 1E*), and similar results were obtained after determining the actual heart weight at necropsy (Supplementary material online, *Figure SIIA*). Lung weights significantly increased only in End.PTP1B-WT mice (Supplementary material online, *Figure SIIB*), consistent with the more severe heart failure in those animals. Of note, none of the above echocardiographical parameters were found to differ significantly between sham-operated End.PTP1B-WT and End.PTP1B-KO mice. Measurement of blood pressure revealed no differences between genotypes ($>n = 12$ mice per group), neither for the systolic (114 ± 4.5 vs. 118 ± 3.7 mmHg; $P = 0.561$) nor for the diastolic blood pressure (76 ± 5.4 vs. 83 ± 3.7 mmHg; $P = 0.272$).

3.3 Absence of PTP1B in endothelial cells prevents cardiac vessel rarefaction and hypoxia after TAC

Histological analysis of serial cross sections through the heart of sham- and TAC-operated mice revealed a significantly smaller mean single cardiomyocyte cross-sectional area (CSA) in the banded hearts of End.PTP1B-KO mice 20 weeks after TAC (representative findings are shown in *Figure 2A* and the summary of the morphometric analysis in *Figure 2B*). A significant reduction in cardiac microvessel density after TAC was observed in End.PTP1B-WT mice but not in their End.PTP1B-KO counterparts (*Figure 2A* and *C*), whereas the number of CD31-immunopositive cells per individual cardiomyocyte was significantly reduced in both genotypes (*Figure 2D*). Cardiac vascularization, as demonstrated by intravital endothelial lectin perfusion, was significantly improved in End.PTP1B-KO compared with End.PTP1B-WT mice (*Figure 2A* and *E*). The higher capillary density was associated with less pronounced tissue hypoxia, as indicated by the lower expression of

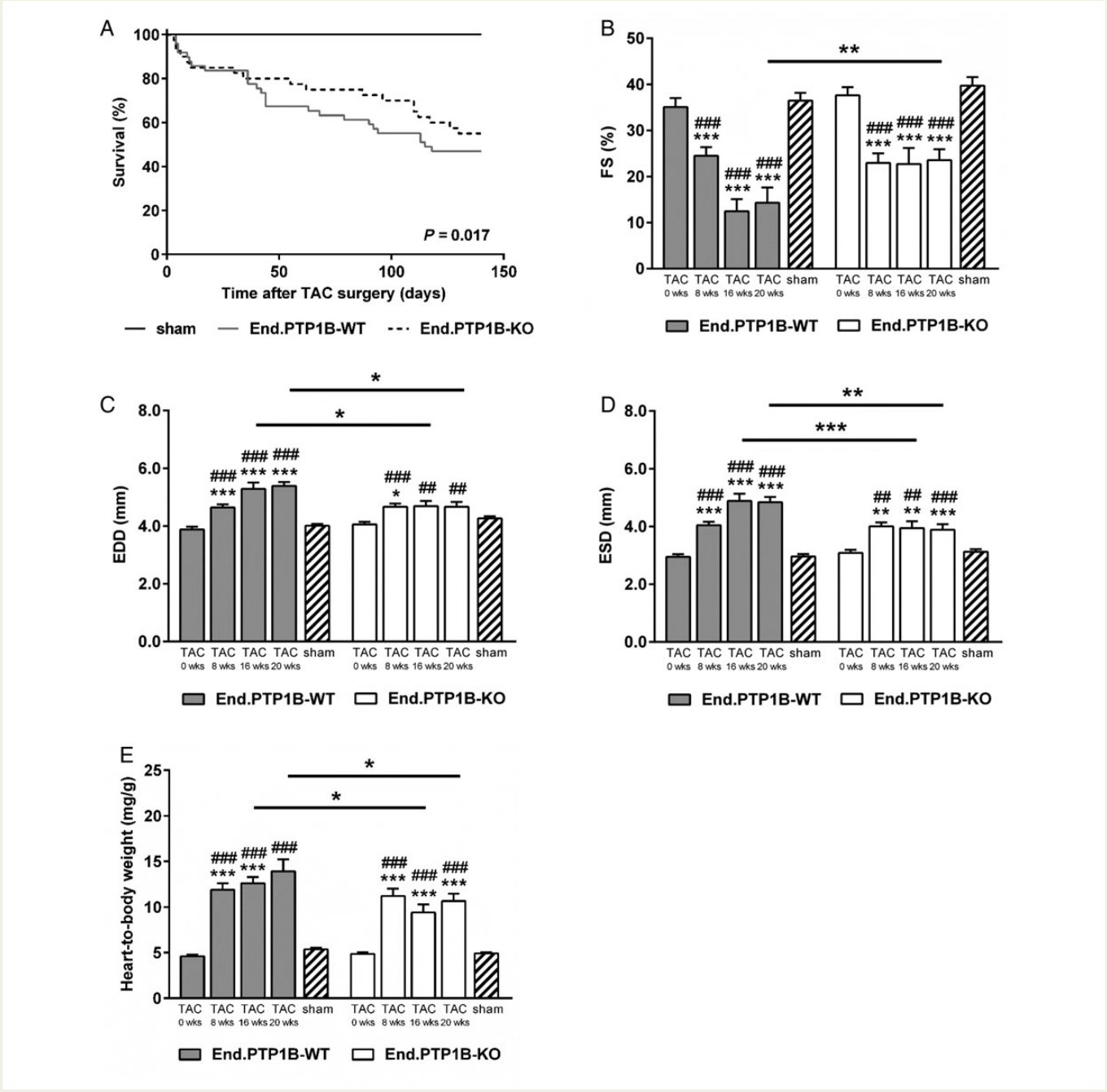

Figure 1 Effect of endothelial PTP1B deletion on survival and cardiac hypertrophy and function. The Kaplan–Meier survival analysis of sham- ($n = 11$) or TAC-operated End.PTP1B-WT ($n = 49$) and End.PTP1B-KO ($n = 40$) mice (*A*). Mean values for FS (*B*), EDDs (*C*), ESDs (*D*), and heart-to-body weight ratio (*E*) determined by echocardiography at baseline ($n = 27$ End.PTP1B-WT and $n = 26$ End.PTP1B-KO mice) and 8 ($n = 27$ End.PTP1B-WT and $n = 26$ End.PTP1B-KO mice), 16 ($n = 10$ End.PTP1B-WT and $n = 12$ End.PTP1B-KO mice), and 20 ($n = 9$ End.PTP1B-WT and $n = 12$ End.PTP1B-KO mice) weeks after TAC or sham operation. $^{*}P < 0.05$, $^{**}P < 0.01$, and $^{***}P < 0.001$ vs. sham, $^{\#\#}P < 0.01$ and $^{\#\#\#}P < 0.001$ vs. baseline. Significant differences between End.PTP1B-WT and End.PTP1B-KO mice are indicated within the graphs.

the HIF transcriptional target CAIX at day 7 after TAC compared with End.PTP1B-WT mice (*Figure 2A* and *F*).

Western blot analysis of total cardiac protein lysates confirmed higher HIF1α protein levels in the hearts from End.PTP1B-WT mice at 7 days after TAC (Supplementary material online, *Figure SIIIA* and *B*). At this time point, significantly increased PTP1B protein levels were observed in End.PTP1B-WT mice but not in their End.PTP1B-KO counterparts (Supplementary material online, *Figure SIIIC* and *D*).

3.4 Endothelial PTP1B deletion improves extra-cardiac angiogenesis

Induction of unilateral hindlimb ischaemia confirmed a significantly improved neovascularization in mice lacking PTP1B in endothelial cells, as shown by serial non-invasive laser Doppler perfusion imaging (*Figure 3A* and *B*) and quantitative CD31 immunostaining of cross sections through the *M. gastrocnemius* harvested 4 weeks after surgery

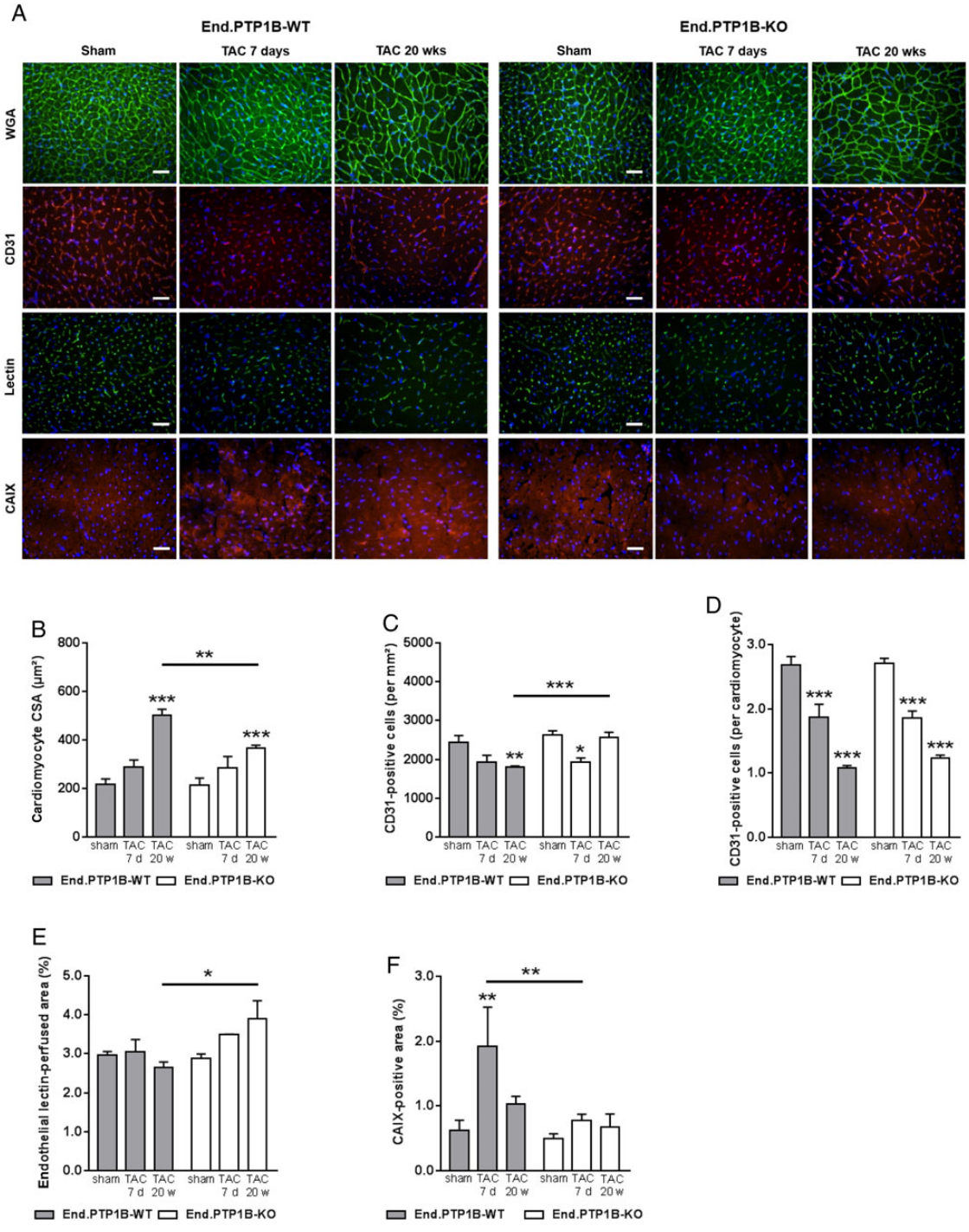

Figure 2 Effect of endothelial PTP1B deletion on single cardiomyocyte hypertrophy, cardiac angiogenesis, and hypoxia. Representative fluorescence microscopy images (*A*) and quantitative analysis of hearts from sham- or TAC-operated End.PTP1B-WT and End.PTP1B-KO mice (at least $n = 5$ per group), after staining with FITC-labelled WGA (*B*), antibodies against CD31 (*C* and *D*), *in vivo* endothelial lectin perfusion (*E*), or antibodies against CAIX (*F*). Size bars represent 100 μm. $^{*}P < 0.05$, $^{**}P < 0.01$, and $^{***}P < 0.001$ vs. sham. Significant differences between End.PTP1B-WT and End.PTP1B-KO mice are indicated within the graphs.

(*Figure 3C* and *D*). Analysis of End.PTP1B-WT mice after sublethal irradiation and transplantation of bone marrow from either End.PTP1B-WT or End.PTP1B-KO mice revealed no differences between both groups (Supplementary material online, *Figure SIVA* and *B*), suggesting that the pro-angiogenic effects of PTP1B do not involve bone marrow-derived cells.

3.5 Deletion of PTP1B in endothelial cells enhances cardiac VEGF signalling

Previous studies have shown that cardiac angiogenesis in response to stress is regulated by VEGF,[3–5] which in endothelial cells signals primarily via VEGFR2.[18] At 20 weeks after TAC, significantly higher levels of

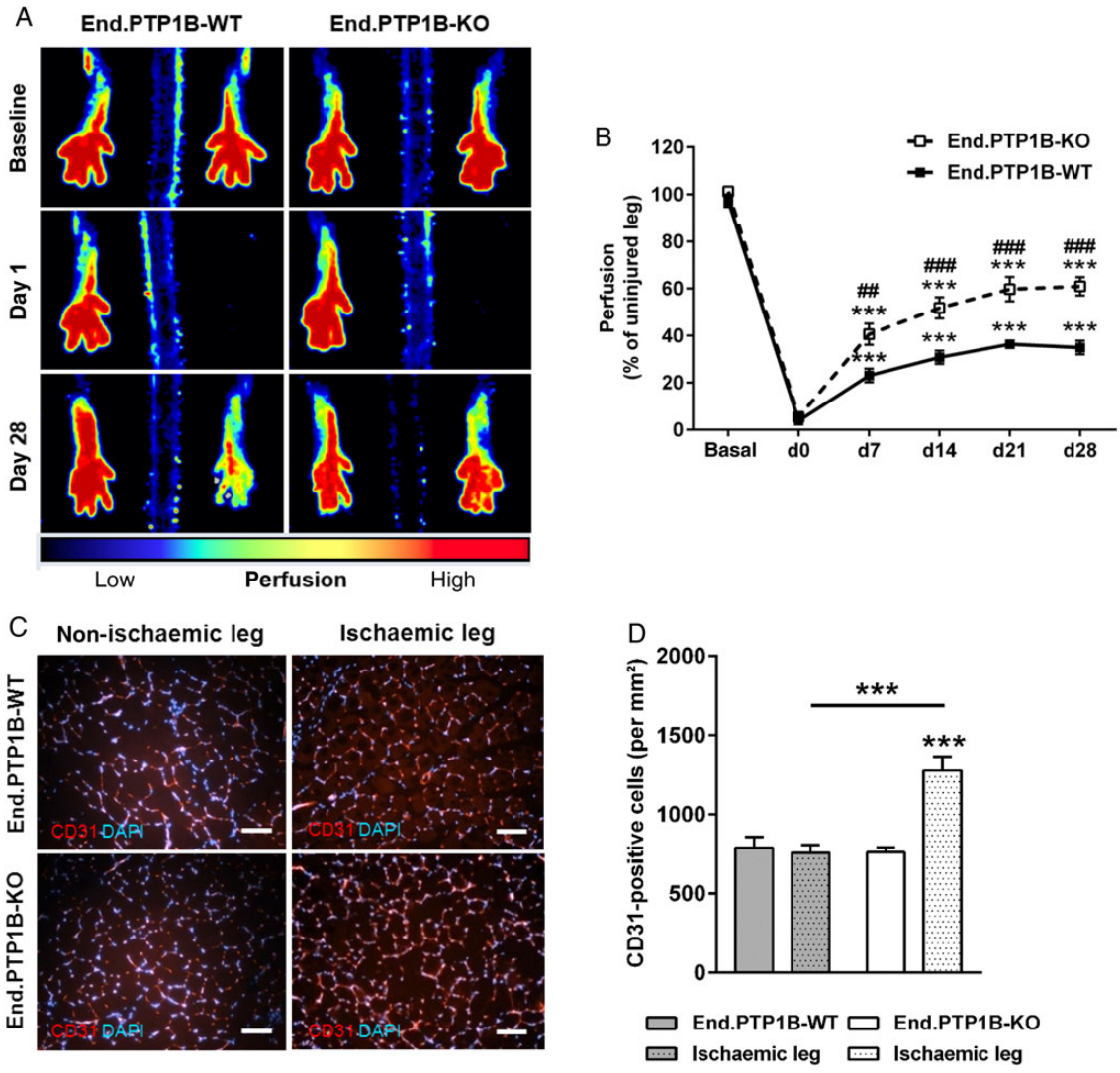

Figure 3 Effect of endothelial PTP1B deletion on neovascularization after hindlimb ischaemia. (*A*) Representative laser Doppler perfusion images before as well as on days 1 and 28 after induction of unilateral hindlimb ischaemia in End.PTP1B-WT and End.PTP1B-KO mice. (*B*) Summarized findings in End.PTP1B-WT ($n = 13$) and End.PTP1B-KO mice ($n = 11$). $^{***}P < 0.001$ vs. day (d) 0; $^{\#\#}P < 0.01$ and $^{\#\#\#}P < 0.001$ vs. End.PTP1B-WT mice. (*C*) Representative images of CD31-immunopositive endothelial cells in cryosections through the gastrocnemic muscle. Cell nuclei were counterstained with DAPI. Size bars represent 100 μm. (D) Quantitative analysis of the capillary density 28 days after ischaemia ($n = 5$ mice per group). $^{***}P < 0.001$ vs. the contralateral, uninjured leg. Significant differences between End.PTP1B-WT and End.PTP1B-KO mice are indicated within the graph.

relative VEGFR2 phosphorylation were observed in the hearts of End.PTP1B-KO mice (*Figure 4A* and *B*). In addition, we examined total and phosphorylated levels of PDGFRβ and FGFR1, i.e. receptors for growth factors involved in cardiac angiogenesis[2] and known to be regulated by PTP1B (i.e. PDGFRβ) or not (FGFR1). These analyses revealed significantly increased levels of total and phosphorylated PDGFRβ in both genotypes at day 7 after TAC, whereas total protein levels increased further only in End.PTP1B-WT but not in End.PTP1B-KO mice ($P < 0.01$ vs. End.PTP1B-KO). This resulted in reduced relative PDGFRβ phosphorylation at 20 W after TAC in End.PTP1B-WT, whereas that in End.PTP1B-KO was not significantly altered (Supplementary material online, *Figure SVA–D*). On the other hand, relative FGFR1 phosphorylation levels did not differ between End.PTP1B-WT and End.PTP1B-KO mice (Supplementary material online, *Figure SVE* and *F*). Consistent with increased VEGFR2 signalling, the hearts of End.PTP1B-KO mice exhibited higher levels of phosphorylated ERK1/2 (*Figure 4C* and *D*). Protein kinase B (AKT) phosphorylation was elevated in both genotypes compared with sham-treated controls, although statistical significance was observed only in mice lacking endothelial PTP1B (*Figure 4E* and *F*). Cardiac total eNOS protein levels also were significantly higher in TAC-operated End.PTP1B-KO mice compared with their End.PTP1B-WT counterparts (*Figure 4G* and *H*), and similar findings were observed for phosphorylated eNOS, resulting in similar relative cardiac phospho-eNOS levels in End.PTP1B-KO and End.PTP1B-WT mice (not shown).

3.6 Endothelial PTP1B deletion enhances cardiac endothelial cell survival after TAC

Based on the above findings of activation of signalling pathways involved in the regulation of cell survival, we next examined

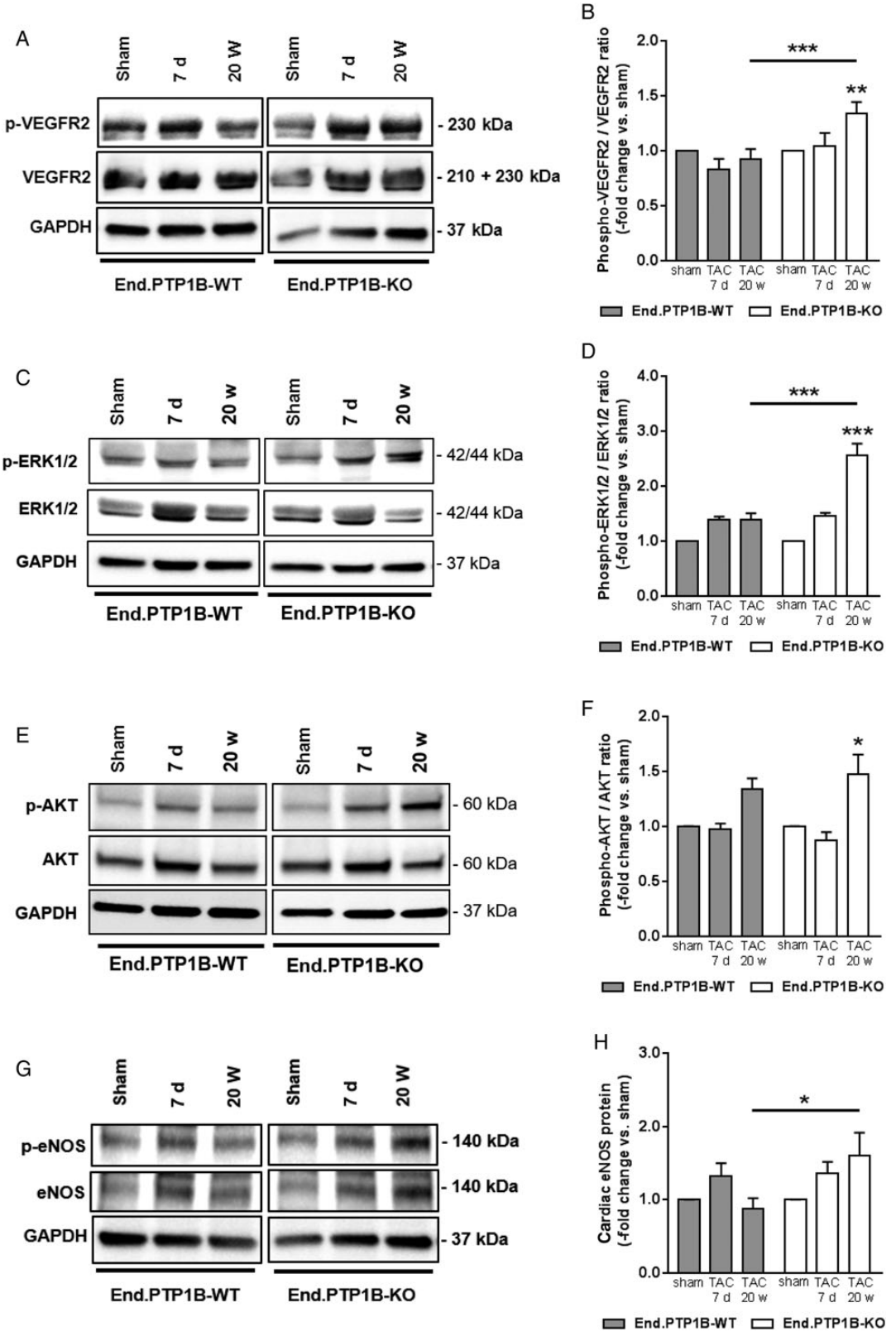

Figure 4 Western blot analysis of cardiac VEGF signalling. Whole heart protein homogenates from sham- and TAC-operated End.PTP1B-WT and End.PTP1B-KO mice were subjected to western blot analysis of phosphorylated VEGFR2 (representative findings in *A*, summarized results in at least $n = 5$ mice per group in *B*), ERK1/2 (*C* and *D*), AKT (*E* and *F*), and eNOS protein expression (*G* and *H*). Results were normalized to GAPDH and are expressed as -fold change vs. sham-operated littermates of the same genotype from the same gel (set at 1). $^{*}P < 0.05$, $^{**}P < 0.01$, and $^{***}P < 0.001$ vs. sham. Significant differences between End.PTP1B-WT and End.PTP1B-KO mice are indicated within the graphs.

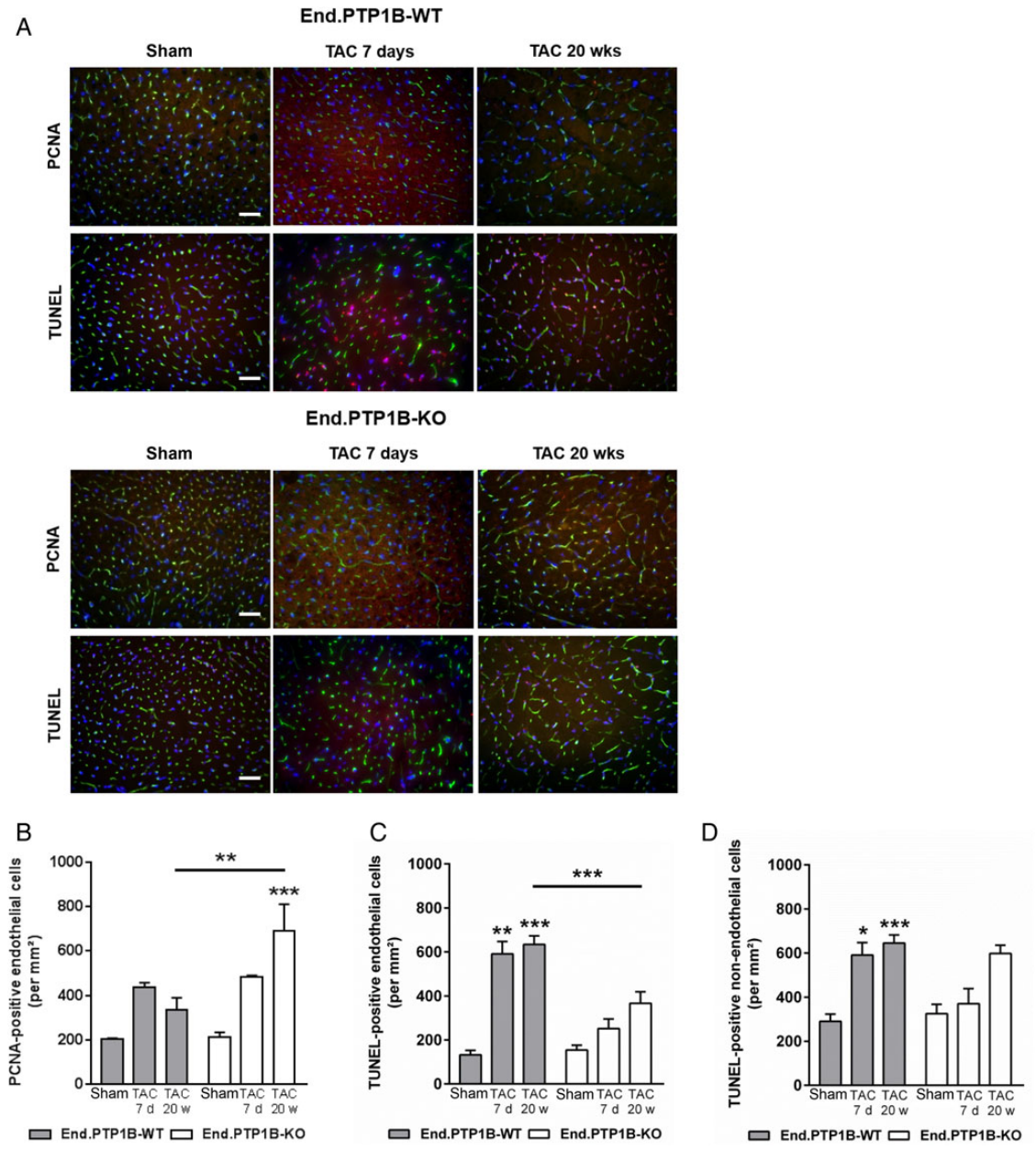

Figure 5 Analysis of cell proliferation and apoptosis in the sham- and TAC-operated mouse hearts. (*A*) Representative images of cardiac cross sections (immuno-)stained for PCNA or TUNEL (red signal). Intravitally isolectin B4-perfused capillaries are marked in green and DAPI-positive cell nuclei in blue. Size bars represent 100 μm. (*B*–*D*) Quantification (at least $n = 6$ mice per group) of the number of PCNA-positive, lectin-positive endothelial cells (*B*), and TUNEL-positive endothelial cells (*C*) or non-endothelial cells (D) per mm^2. *$P < 0.05$ and ***$P < 0.001$ vs. sham. Significant differences between End.PTP1B-WT and End.PTP1B-KO mice are indicated within the graphs.

whether endothelial deletion of PTP1B alters cardiac proliferation and apoptosis after TAC. Histochemical analysis revealed higher numbers of PCNA-positive, proliferating endothelial cells in the End.PTP1B-KO mouse hearts (*Figure 5A* and *B*), whereas the number of TUNEL-positive apoptotic cells, dual-positive for endothelial lectin, was found to be reduced (*Figure 5A* and *C*). On the other hand, the number of TUNEL-positive non-endothelial cells was increased to a similar extent in both genotypes, although changes did not reach statistical significance in End.PTP1B-KO mice (*Figure 5A* and *D*).

3.7 Endothelial PTP1B deletion upregulates endothelial caveolin-1 expression and ameliorates oxidative stress

Histological analysis confirmed increased cardiac expression of eNOS in mice lacking PTP1B in endothelial cells (*Figure 6A* and *B*). As VEGFR2 and eNOS are both localized in caveolae and as PTP1B may bind to caveolin-1, the principal structural component of caveolae in endothelial cells, we next examined cardiac caveolin-1 expression levels. Histological analysis revealed elevated expression of caveolin-1 in the hearts of End.PTP1B-KO mice 20 weeks after TAC (*Figure 6A* and *C*), and

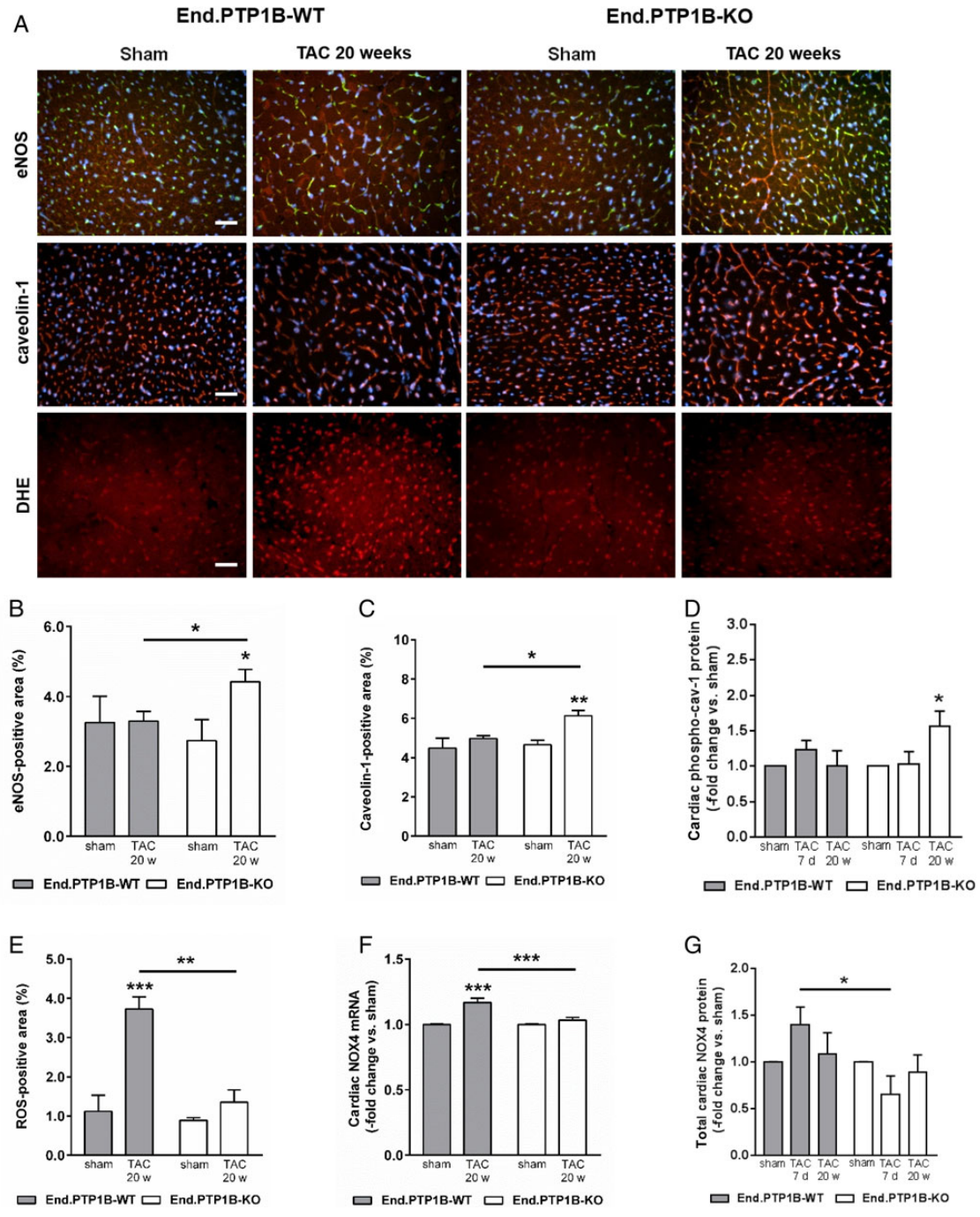

Figure 6 Effect of endothelial PTP1B deletion on cardiac eNOS, caveolin-1, and ROS levels. (*A*) Cryosections through the sham- or TAC-operated End.PTP1B-WT and End.PTP1B-KO hearts were immunostained for eNOS (red signal; quantitative analysis in *B*; $n = 5$ mice per group) or caveolin-1 (red signal; quantitative analysis in *C*; $n = 6$ mice per group). Intravitally isolectin B4-perfused capillaries are marked in green, DAPI-positive cell nuclei in blue. Size bars represent 100 μm. Phosphorylated caveolin-1 protein levels were detected using western blot of whole mouse heart homogenates (*D*; at least 5 mice per group). *In vivo* ROS generation was visualized using DHE (red signal; quantitative analysis in *E*; $n = 3$ mice per group). NOX4 expression was examined on the mRNA (*F*; $n = 6$ mice per group) and the protein (*G*; at least 5 mice per group) levels. $^{*}P < 0.05$, $^{**}P < 0.001$, and $^{***}P < 0.001$ vs. sham. Significant differences between End.PTP1B-WT and End.PTP1B-KO mice are indicated within the graphs.

western blot analysis confirmed higher phosphorylated caveolin-1 protein expression levels in the End.PTP1B-KO mouse hearts (*Figure 6D*). On the other hand, immunofluorescence imaging of DHE revealed lower levels of ROS production in the End.PTP1B-KO mouse hearts (*Figure 6A* and *E*). In line with these findings, cardiac mRNA (*Figure 6F*) and protein (*Figure 6G*) expression of the endothelial NADPH isoform NOX4 was found to be reduced in End.PTP1B-KO compared with End.PTP1B-WT mice.

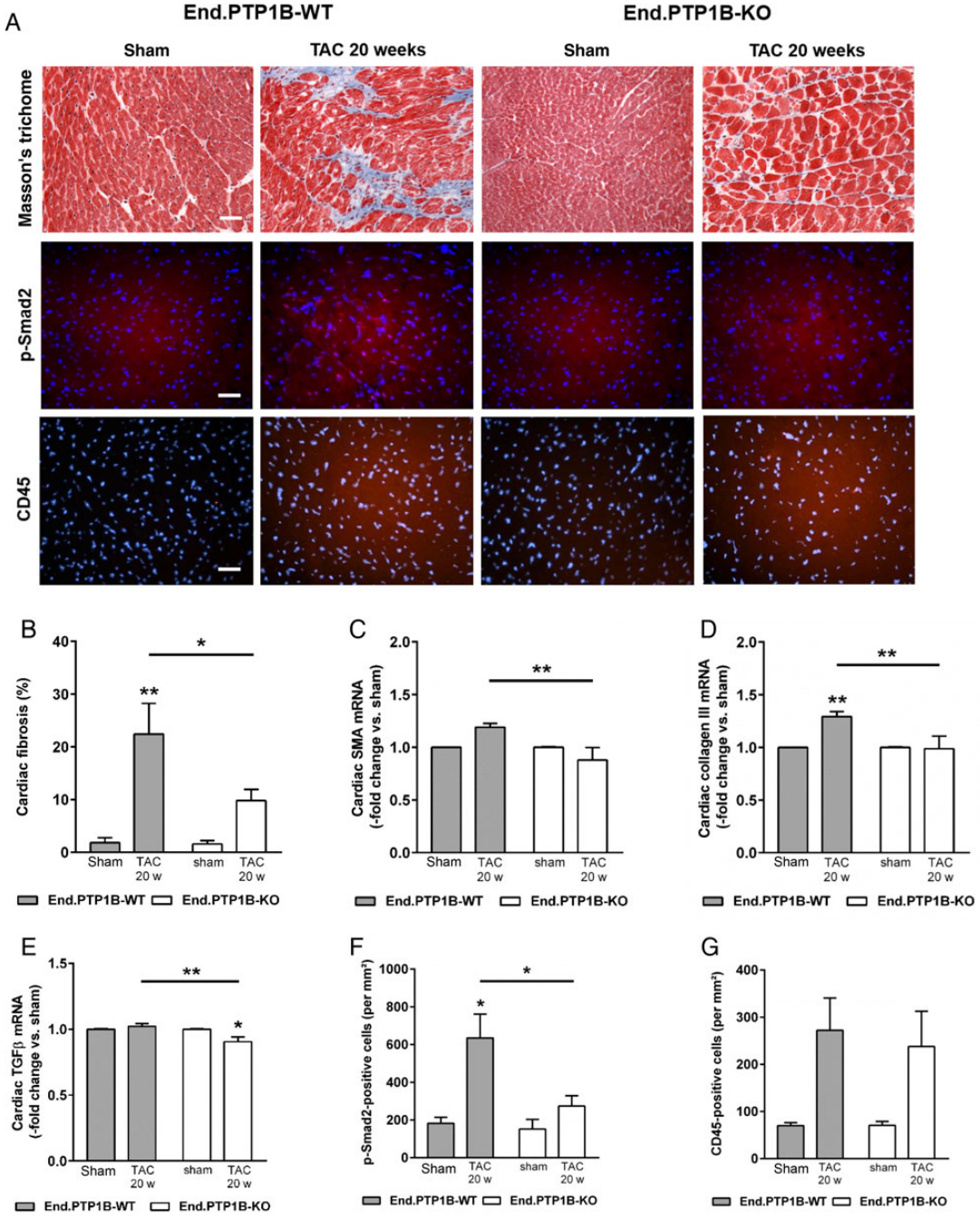

Figure 7 Effect of endothelial PTP1B deletion on cardiac fibrosis and TGFβ signalling. (*A*) Representative images after MTC or p-Smad2 and CD45 (immuno-)staining of the hearts from End.PTP1B-WT and End.PTP1B-KO mice. Size bars represent 100 μm. Summary of the quantitative analysis in at least $n = 7$ mice per group for MTC (*B*), p-Smad2 (*F*), and CD45 (*G*). (*C*–*E*) qPCR analysis (at least $n = 6$ mice per group) of the mRNA expression of smooth muscle actin (SMA) (*C*), collagen III (*D*), and TGFβ (*E*). Results were normalized to GAPDH and are expressed as -fold change vs. sham-operated mice (set at 1). $^{*}P < 0.05$ and $^{**}P < 0.01$ vs. sham. Significant differences between End.PTP1B-WT and End.PTP1B-KO mice are indicated within the graphs.

3.8 Endothelial PTP1B deletion reduces cardiac fibrosis after TAC

Analysis of cardiac fibrosis 20 weeks after TAC using MTC staining revealed more pronounced extracellular matrix deposition in the hearts of End.PTP1B-WT mice (*Figure 7A* and *B*). Similar findings were obtained after sirius red staining for interstitial collagen (not shown). In line with these findings, qPCR revealed significantly lower mRNA expression levels of SMA (*Figure 7C*), collagen III (*Figure 7D*), and TGFβ (*Figure 7E*) in the hearts of End.PTP1B-KO mice compared with their End.PTP1B-WT counterparts. Cardiac levels of phosphorylated Smad2, indicating activated TGFβ signalling, were significantly elevated in End.PTP1B-WT mice but not in End.PTP1B-KO animals (*Figure 7A* and *F*). Of note, the number of CD45-positive inflammatory cells was increased to a similar extent in the banded hearts of both genotypes (*Figure 7A* and *G*).

4. Discussion

In this study, we examined the importance of PTP1B expression in endothelial cells for cardiac angiogenesis and remodelling processes during chronic pressure overload-induced hypertrophy. We could show that endothelial deletion of PTP1B promotes cardiac and extracardiac angiogenesis and reduces cardiac hypoxia, oxidative stress, and fibrosis, resulting in improved survival and less pronounced echocardiographic signs of heart failure. We demonstrate that endothelial PTP1B deletion was associated with enhanced cardiac VEGF signalling and improved endothelial survival. Moreover, elevated levels of caveolin-1 may have contributed to the protection from cardiac fibrosis and heart failure by reducing oxidative stress and TGFβ signalling.

Cardiomyocyte hypertrophy is initially associated with increased angiogenesis, whereas a rarefaction of the cardiac microvasculature is observed at later stages and may contribute to the progression from adaptive remodelling towards heart failure.[19] Inhibition of blood vessel formation was shown to accelerate the development of cardiac dysfunction,[3,5] whereas angiogenesis stimulation delayed the onset of heart failure.[20] Whereas the role of VEGF and other angiogenic growth factors for cardiac angiogenesis has been intensively studied,[3–5] the molecular mediators involved in cardiac vessel reduction during pathological hypertrophy are largely unknown. In addition to an inadequate expression of angiogenic growth factors by hypertrophied cardiomyocytes, up-regulation of counterregulatory mediators and resistance towards angiogenic growth factor stimulation may also play a role. In this respect, PTP1B represents an interesting candidate. In a genome-wide gene expression analysis, we have previously shown that increased cardiac afterload is, among others, associated with elevated expression of counterregulatory phosphatases, including PTP1B,[15] and these results were confirmed in the present study. The almost complete abolishment of PTP1B overexpression in the banded hearts of End.PTP1B-KO mice suggests a major contribution of endothelial cells to this observation. Regarding the stimuli underlying cardiac/endothelial PTP1B overexpression in chronic pressure overload, cardiac PTP1B overexpression coincided with elevated HIF1α protein, suggesting that cardiac hypoxia may have played a role. Previous studies have found markedly elevated active PTP1B protein levels in ischaemic hindlimb muscles.[9]

PTP1B inhibition or silencing was shown to enhance the VEGF-induced migration and proliferation of mouse heart microvascular endothelial cells.[21] The general phosphatase blocker sodium orthovanadate increased VEGFR2 and AKT phosphorylation and accelerated angiogenesis in a rat model of hindlimb ischaemia,[22] and similar findings were observed using the non-selective PTP inhibitor bis(maltolato)oxovanadium IV.[23] Recently, endothelial PTP1B was demonstrated to regulate VEGF-induced angiogenesis and arteriogenesis under physiological conditions.[10] We had shown that the non-responsiveness of endothelial progenitor cells from obese individuals to angiogenic growth factor stimulation involves endothelial overexpression of PTP1B.[16] With regard to cardiac pathologies, systemic pharmacological inhibition or genetic deletion of PTP1B was shown to protect mice against chronic heart failure induced by myocardial infarction.[11,21] This was accompanied by reduced cardiac fibrosis and cardiomyocyte hypertrophy and also ameliorated the endothelial dysfunction associated with heart failure,[11] possibly through restoration of eNOS phosphorylation in peripheral resistance arteries.[12] PTP1B deficiency also was found to protect against acute heart failure in mouse models of lipopolysaccharide- or caecal puncture-induced heart failure.[24] On the other hand, the role of PTP1B during chronic pressure overload-induced cardiac hypertrophy and heart failure has not been examined thus far. In the present study, we could show that endothelial PTP1B deletion promotes cardiac vascularization and prevents cardiac decompensation, hypoxia, and fibrosis, ultimately protecting mice against heart failure induced by chronically increased cardiac afterload. Although findings between different studies and models may not be directly comparable, the observed beneficial effects in mice with endothelial-specific PTP1B deletion in terms of improvement of systolic pump function were very similar to those observed in mice with systemic gene deletion or after pharmacological inhibition and ischaemia-induced heart failure,[11] underlining the importance of PTP1B expressed in endothelial cells for the cardiac response to injury.

The anti-angiogenic effects of PTP1B have been primarily explained by dephosphorylation of VEGFR2 and subsequent reduction of ERK1/2 activation and endothelial cell proliferation.[9,10] Our findings confirm enhanced cardiac VEGFR2 signalling, whereas the relative phosphorylation of receptors for other growth factors involved in cardiac angiogenesis (such as PDGF and FGF2) was found not to differ between genotypes. Interestingly, total PDGFRβ protein expression significantly increased at 7 days after TAC, in line with previous findings,[25] but further increased only in End.PTP1B-WT mice, possibly underlining the more pronounced TAC-induced cardiomyocyte stress in those mice. Moreover, elevated levels of proliferating endothelial cells and functional, i.e. perfused vessels were observed in the banded hearts of mice lacking endothelial PTP1B, and cardiac endothelial cell apoptosis was found to be reduced, which may have contributed to the observed stabilization of the cardiac microvasculature in endothelial PTP1B-deficient mice. Previous studies have implicated PTP1B in apoptosis: PTP1B deficiency in hepatocytes was shown to confer resistance to apoptosis by altering the balance of pro- and anti-apoptotic members of the Bcl-2 family.[26] Small interference RNA against PTP1B reduced FasR-induced caspase-3 and caspase-8 activation following exposure of neonatal rat cardiac myocytes to hypoxia reoxygenation.[27]

A major finding of the present study is the significant reduction of cardiac fibrosis in mice lacking PTP1B in endothelial cells. One potential explanation may be the improved angiogenesis due to enhanced VEGF signalling, as shown by the increased activation of the downstream angiogenic mediators eNOS or ERK1/2. The subsequent improvement of cardiac perfusion and reduction of hypoxia may have indirectly contributed to reduced cardiac cell death and replacement fibrosis, in addition to direct effects of PTP1B on apoptotic cell death, as discussed above. We did not observe any differences in cardiac COX2 mRNA and protein expression levels between both genotypes, as recently reported in plasma of mice with streptozotocin-induced type 1 diabetes and found to underlie the protection against endothelial dysfunction.[28] Differences in fibrosis secondary to altered levels of cardiac inflammation may also have been involved, as a recent study found that systemic PTP1B deficiency was associated with elevated numbers of cardiac M2 macrophages after myocardial infarction.[21] In this regard, we observed a similar increase in CD45-positive leucocytes in both genotypes 20 weeks after TAC, although the time point might have been too late to detect any differences. Of note, PTP1B expressed in haematopoietic cells derived from the bone marrow did not play a major role, at least not for the angiogenic phenotype examined after induction of peripheral ischaemia.

PTP1B is known to physically associate with caveolin-1, a major component of caveolae, lipid-rich cell membrane invaginations involved in the structural and functional organization of transmembrane receptors. Caveolin-1 is primarily expressed in endothelial cells and fibroblasts

and regulates, among others, the activity of VEGFR2 and eNOS. Rather surprisingly, in the present study, we observed an increased cardiac expression of caveolin-1 in mice lacking PTP1B. Phosphorylated caveolin-1 levels also were significantly increased, although phosphocaveolin has been identified as potential PTP1B substrate.[29] The mechanisms underlying this observation have to be explored in more detail in future studies. Several studies have shown that caveolin-1 inhibits eNOS enzyme activity and NO formation in endothelial cells.[30] Although reduced NO production may be undesirable in acute situations, the caveolin-1–NO interaction may protect from chronic NO-derived superoxide anion generation following persistent eNOS activation, substrate depletion, and eNOS uncoupling. In line with this notion, endothelial cells lacking caveolin-1 exhibited increased levels of intracellular H_2O_2 and mitochondrial ROS production.[31] Caveolin-1 deficient mice develop cardiac hypertrophy and fibrosis,[32] possibly due to constitutive hyperactivation of the NO pathway and enhanced radical stress.[33] Mechanistically, caveolin-1 has been shown to reduce ROS production in pulmonary artery endothelial cells by repressing the expression of NOX2 and NOX4.[34] In line with the observed increased cardiac caveolin-1 expression, the hearts of End.PTP1B-KO mice exhibited reduced ROS production, as shown by DHE staining, and significantly lower levels of NOX4 mRNA and protein expression may have contributed to this observation. In addition to inhibiting ROS generation, caveolin-1 possesses anti-fibrotic properties and has been shown to suppress TGFβ1-induced extracellular matrix production in cultured fibroblasts,[35] possibly via TGFβ receptor internalization through lipid rafts.[36] To this end, lower levels of phosphorylated Smad2 were observed in the hearts of End.PTP1B-KO mice, which may have contributed to the reduced levels of cardiac apoptosis and fibrosis and protection from heart failure.

Taken together, our findings suggest that endothelial PTP1B is important for the rarefaction of the cardiac microvasculature during chronic afterload-induced hypertrophy, possibly by inhibiting VEGF signal transduction resulting in decreased eNOS synthesis and ERK1/2 activation, reduced endothelial proliferation, and enhanced apoptosis. The subsequent reduction in cardiac perfusion and increase in tissue hypoxia, but also down-regulation of caveolin-1 with a subsequent increase in NOX4 expression, ROS generation, and TGFβ signalling may have contributed to the development of cardiac fibrosis, the histological substrate of heart failure.

Supplementary material

Supplementary material is available at *Cardiovascular Research* online.

Acknowledgements

We thank Benjamin G. Neel (University Health Network, Toronto, ON, Canada) for providing the $PTP1B^{fl/fl}$ mice and Bernd Arnold (German Cancer Research Center, DKFZ, Heidelberg, Germany) for providing the Tie2.ERT2.Cre mice. We are also grateful for the support provided by the EC FP7 Capacities Specific Program-funded EMMA service project. The authors acknowledge the expert technical assistance of Kirsten Koschel, Frauke Dormann, and Sarah Zafar.

Conflict of interest: none declared.

Funding

This work was supported by grants from the German Research Foundation [*Deutsche Forschungsgemeinschaft*; SFB 1002 (Teilprojekt C06)] and the intramural research funding of the University Medical Center Mainz to K.S.

References

1. Billinger M, Kloos P, Eberli FR, Windecker S, Meier B, Seiler C. Physiologically assessed coronary collateral flow and adverse cardiac ischemic events: a follow-up study in 403 patients with coronary artery disease. *J Am Coll Cardiol* 2002;**40**:1545–1550.
2. Hudlicka O, Brown M, Egginton S. Angiogenesis in skeletal and cardiac muscle. *Physiol Rev* 1992;**72**:369–417.
3. Giordano FJ, Gerber HP, Williams SP, VanBruggen N, Bunting S, Ruiz-Lozano P, Gu Y, Nath AK, Huang Y, Hickey R, Dalton N, Peterson KL, Ross J Jr., Chien KR, Ferrara N. A cardiac myocyte vascular endothelial growth factor paracrine pathway is required to maintain cardiac function. *Proc Natl Acad Sci U S A* 2001;**98**:5780–5785.
4. May D, Gilon D, Djonov V, Itin A, Lazarus A, Gordon O, Rosenberger C, Keshet E. Transgenic system for conditional induction and rescue of chronic myocardial hibernation provides insights into genomic programs of hibernation. *Proc Natl Acad Sci U S A* 2008;**105**:282–287.
5. Izumiya Y, Shiojima I, Sato K, Sawyer DB, Colucci WS, Walsh K. Vascular endothelial growth factor blockade promotes the transition from compensatory cardiac hypertrophy to failure in response to pressure overload. *Hypertension* 2006;**47**:887–893.
6. Abraham D, Hofbauer R, Schafer R, Blumer R, Paulus P, Miksovsky A, Traxler H, Kocher A, Aharinejad S. Selective downregulation of VEGF-A(165), VEGF-R(1), and decreased capillary density in patients with dilative but not ischemic cardiomyopathy. *Circ Res* 2000;**87**:644–647.
7. Kaza E, Ablasser K, Poutias D, Griffiths ER, Saad FA, Hofstaetter JG, del Nido PJ, Friehs I. Up-regulation of soluble vascular endothelial growth factor receptor-1 prevents angiogenesis in hypertrophied myocardium. *Cardiovasc Res* 2011;**89**:410–418.
8. Nakamura T, Funayama H, Kubo N, Yasu T, Kawakami M, Momomura S, Ishikawa SE. Elevation of plasma placental growth factor in the patients with ischemic cardiomyopathy. *Int J Cardiol* 2009;**131**:186–191.
9. Nakamura Y, Patrushev N, Inomata H, Mehta D, Urao N, Kim HW, Razvi M, Kini V, Mahadev K, Goldstein BJ, McKinney R, Fukai T, Ushio-Fukai M. Role of protein tyrosine phosphatase 1B in vascular endothelial growth factor signaling and cell-cell adhesions in endothelial cells. *Circ Res* 2008;**102**:1182–1191.
10. Lanahan AA, Lech D, Dubrac A, Zhang J, Zhuang ZW, Eichmann A, Simons M. PTP1b is a physiologic regulator of vascular endothelial growth factor signaling in endothelial cells. *Circulation* 2014;**130**:902–909.
11. Gomez E, Vercauteren M, Kurtz B, Ouvrard-Pascaud A, Mulder P, Henry JP, Besnier M, Waget A, Hooft van HR, Tremblay ML, Burcelin R, Thuillez C, Richard V. Reduction of heart failure by pharmacological inhibition or gene deletion of protein tyrosine phosphatase 1B. *J Mol Cell Cardiol* 2012;**52**:1257–1264.
12. Vercauteren M, Remy E, Devaux C, Dautreaux B, Henry JP, Bauer F, Mulder P, Hooft van HR, Bombrun A, Thuillez C, Richard V. Improvement of peripheral endothelial dysfunction by protein tyrosine phosphatase inhibitors in heart failure. *Circulation* 2006;**114**:2498–2507.
13. Bence KK, Delibegovic M, Xue B, Gorgun CZ, Hotamisligil GS, Neel BG, Kahn BB. Neuronal PTP1B regulates body weight, adiposity and leptin action. *Nat Med* 2006;**12**:917–924.
14. Forde A, Constien R, Grone HJ, Hammerling G, Arnold B. Temporal Cre-mediated recombination exclusively in endothelial cells using Tie2 regulatory elements. *Genesis* 2002;**33**:191–197.
15. Toischer K, Rokita AG, Unsold B, Zhu W, Kararigas G, Sossalla S, Reuter SP, Becker A, Teucher N, Seidler T, Grebe C, Preuss L, Gupta SN, Schmidt K, Lehnart SE, Krüger M, Linke WA, Backs J, Regitz-Zagrosek V, Schäfer K, Field LJ, Maier LS, Hasenfuss G. Differential cardiac remodeling in preload versus afterload. *Circulation* 2010;**122**:993–1003.
16. Heida NM, Leifheit-Nestler M, Schroeter MR, Müller JP, Cheng IF, Henkel S, Limbourg A, Limbourg FP, Alves F, Quigley JP, Ruggeri ZM, Hasenfuss G, Konstantinides S, Schäfer K. Leptin enhances the potency of circulating angiogenic cells via src kinase and integrin (alpha)vbeta5: implications for angiogenesis in human obesity. *Arterioscler Thromb Vasc Biol* 2010;**30**:200–206.
17. Schroeter MR, Stein S, Heida NM, Leifheit-Nestler M, Cheng IF, Gogiraju R, Christiansen H, Maier LS, Shah AM, Hasenfuss G, Konstantinides S, Schäfer K. Leptin promotes the mobilization of vascular progenitor cells and neovascularization by NOX2-mediated activation of MMP9. *Cardiovasc Res* 2012;**93**:170–180.
18. Olsson AK, Dimberg A, Kreuger J, Claesson-Welsh L. VEGF receptor signalling – in control of vascular function. *Nat Rev Mol Cell Biol* 2006;**7**:359–371.
19. Hein S, Arnon E, Kostin S, Schonburg M, Elsasser A, Polyakova V, Bauer EP, Klovekorn WP, Schaper J. Progression from compensated hypertrophy to failure in the pressure-overloaded human heart: structural deterioration and compensatory mechanisms. *Circulation* 2003;**107**:984–991.
20. Friehs I, Margossian RE, Moran AM, Cao-Danh H, Moses MA, del Nido PJ. Vascular endothelial growth factor delays onset of failure in pressure-overload hypertrophy through matrix metalloproteinase activation and angiogenesis. *Basic Res Cardiol* 2006;**101**:204–213.
21. Besnier M, Galaup A, Nicol L, Henry JP, Coquerel D, Gueret A, Mulder P, Brakenhielm E, Thuillez C, Germain S, Richard V, Ouvrard-Pascaud A. Enhanced

angiogenesis and increased cardiac perfusion after myocardial infarction in protein tyrosine phosphatase 1B-deficient mice. *FASEB J* 2014;**28**:3351–3361.
22. Sugano M, Tsuchida K, Makino N. A protein tyrosine phosphatase inhibitor accelerates angiogenesis in a rat model of hindlimb ischemia. *J Cardiovasc Pharmacol* 2004;**44**: 460–465.
23. Carr AN, Davis MG, Eby-Wilkens E, Howard BW, Towne BA, Dufresne TE, Peters KG. Tyrosine phosphatase inhibition augments collateral blood flow in a rat model of peripheral vascular disease. *Am J Physiol Heart Circ Physiol* 2004;**287**:H268–H276.
24. Coquerel D, Neviere R, Delile E, Mulder P, Marechal X, Montaigne D, Renet S, Remy-Jouet I, Gomez E, Henry JP, do Rego JC, Richard V, Tamion F. Gene deletion of protein tyrosine phosphatase 1B protects against sepsis-induced cardiovascular dysfunction and mortality. *Arterioscler Thromb Vasc Biol* 2014;**34**:1032–1044.
25. Chintalgattu V, Ai D, Langley RR, Zhang J, Bankson JA, Shih TL, Reddy AK, Coombes KR, Daher IN, Pati S, Patel SS, Pocius JS, Taffet GE, Buja LM, Entman ML, Khakoo AY. Cardiomyocyte PDGFR-beta signaling is an essential component of the mouse cardiac response to load-induced stress. *J Clin Invest* 2010;**120**:472–484.
26. Gonzalez-Rodriguez A, Escribano O, Alba J, Rondinone CM, Benito M, Valverde AM. Levels of protein tyrosine phosphatase 1B determine susceptibility to apoptosis in serum-deprived hepatocytes. *J Cell Physiol* 2007;**212**:76–88.
27. Song H, Zhang Z, Wang L. Small interference RNA against PTP-1B reduces hypoxia/reoxygenation induced apoptosis of rat cardiomyocytes. *Apoptosis* 2008;**13**:383–393.
28. Herren DJ, Norman JB, Anderson R, Tremblay ML, Huby AC, Belin de Chantemèle EJ. Deletion of Protein Tyrosine Phosphatase 1B (PTP1B) enhances endothelial cyclooxygenase 2 expression and protects mice from type 1 diabetes-induced endothelial dysfunction. *PLoS One* 2015;**10**:e0126866.
29. Lee H, Xie L, Luo Y, Lee SY, Lawrence DS, Wang XB, Sotgia F, Lisanti MP, Zhang ZY. Identification of phosphocaveolin-1 as a novel protein tyrosine phosphatase 1B substrate. *Biochemistry* 2006;**45**:234–240.
30. Feron O, Dessy C, Moniotte S, Desager JP, Balligand JL. Hypercholesterolemia decreases nitric oxide production by promoting the interaction of caveolin and endothelial nitric oxide synthase. *J Clin Invest* 1999;**103**:897–905.
31. Shiroto T, Romero N, Sugiyama T, Sartoretto JL, Kalwa H, Yan Z, Shimokawa H, Michel T. Caveolin-1 is a critical determinant of autophagy, metabolic switching, and oxidative stress in vascular endothelium. *PLoS One* 2014;**9**:e87871.
32. Cohen AW, Park DS, Woodman SE, Williams TM, Chandra M, Shirani J, Pereira de SA, Kitsis RN, Russell RG, Weiss LM, Tang B, Jelicks LA, Factor SM, Shtutin V, Tanowitz HB, Lisanti MP. Caveolin-1 null mice develop cardiac hypertrophy with hyperactivation of p42/44 MAP kinase in cardiac fibroblasts. *Am J Physiol Cell Physiol* 2003;**284**: C457–C474.
33. Wunderlich C, Schober K, Kasper M, Heerwagen C, Marquetant R, Ebner B, Forkmann M, Schoen S, Braun-Dullaeus RC, Schmeisser A, Strasser RH. Nitric oxide synthases are crucially involved in the development of the severe cardiomyopathy of caveolin-1 knockout mice. *Biochem Biophys Res Commun* 2008;**377**:769–774.
34. Chen F, Barman S, Yu Y, Haigh S, Wang Y, Black SM, Rafikov R, Dou H, Bagi Z, Han W, Su Y, Fulton DJ. Caveolin-1 is a negative regulator of NADPH oxidase-derived reactive oxygen species. *Free Radic Biol Med* 2014;**73**:201–213.
35. Wang XM, Zhang Y, Kim HP, Zhou Z, Feghali-Bostwick CA, Liu F, Ifedigbo E, Xu X, Oury TD, Kaminski N, Choi AM. Caveolin-1: a critical regulator of lung fibrosis in idiopathic pulmonary fibrosis. *J Exp Med* 2006;**203**:2895–2906.
36. Di Guglielmo GM, Le RC, Goodfellow AF, Wrana JL. Distinct endocytic pathways regulate TGF-beta receptor signalling and turnover. *Nat Cell Biol* 2003;**5**:410–421.